



WILLIAM & MARY

CHARTERED 1693

W&M ScholarWorks

VIMS Articles

Virginia Institute of Marine Science

2-2021

Coastal Forest Seawater Exposure Increases Stem Methane Concentration

Matthew J. Norwood

Nicholas Ward

(.....)

Matthew Kirwan

Virginia Institute of Marine Science

Anya Hopple

See next page for additional authors

Follow this and additional works at: <https://scholarworks.wm.edu/vimsarticles>

 Part of the [Earth Sciences Commons](#)

Recommended Citation

Norwood, Matthew J.; Ward, Nicholas; (.....); Kirwan, Matthew; Hopple, Anya; and Megonigal, J. Patrick, *Coastal Forest Seawater Exposure Increases Stem Methane Concentration* (2021). *JGR Biogeosciences*, 126(2), e2020JG005915.

doi: 10.1029/2020JG005915

This Article is brought to you for free and open access by the Virginia Institute of Marine Science at W&M ScholarWorks. It has been accepted for inclusion in VIMS Articles by an authorized administrator of W&M ScholarWorks. For more information, please contact scholarworks@wm.edu.

Authors

Matthew J. Norwood, Nicholas Ward, (.....), Matthew Kirwan, Anya Hopple, and J. Patrick Megonigal

JGR Biogeosciences

RESEARCH ARTICLE

10.1029/2020JG005915

Key Points:

- Seawater exposure significantly increased internal stem CH_4 concentration
- There is a significant correlation between stem wood density and stem CH_4 concentration
- Low stem and soil O_2 were significantly linked to seawater exposure and decreased tree survival

Supporting Information:

- Supporting Information S1

Correspondence to:

M. J. Norwood,
matthew.norwood@pnnl.gov

Citation:

Norwood, M. J., Ward, N. D., McDowell, N. G., Myers-Pigg, A. N., Bond-Lamberty, B., Indivero, J., et al. (2021). Coastal forest seawater exposure increases stem methane concentration. *Journal of Geophysical Research: Biogeosciences*, 126, e2020JG005915. <https://doi.org/10.1029/2020JG005915>

Received 16 JUN 2020

Accepted 21 DEC 2020

Author Contributions:

Conceptualization: Matthew J. Norwood, Nicholas D. Ward
Data curation: Matthew J. Norwood
Formal analysis: Matthew J. Norwood
Funding acquisition: Nicholas D. Ward
Investigation: Matthew J. Norwood, Nicholas D. Ward, Allison N. Myers-Pigg, Ben Bond-Lamberty, Julia Indivero, Stephanie Pennington, Wenzhi Wang, Matt Kirwan
Methodology: Matthew J. Norwood, Nicholas D. Ward
Project Administration: Nicholas D. Ward
Supervision: Nicholas D. Ward, Nate G. McDowell, J. Patrick Megonigal
Writing – original draft: Matthew J. Norwood, Nicholas D. Ward, Nate G. McDowell, Allison N. Myers-Pigg, Ben Bond-Lamberty, Julia Indivero, Stephanie Pennington, Wenzhi Wang

© 2020. American Geophysical Union.
All Rights Reserved.

Coastal Forest Seawater Exposure Increases Stem Methane Concentration

Matthew J. Norwood¹ , Nicholas D. Ward^{1,2} , Nate G. McDowell^{3,4},
Allison N. Myers-Pigg^{1,5} , Ben Bond-Lamberty⁶ , Julia Indivero^{1,7} ,
Stephanie Pennington⁶ , Wenzhi Wang^{3,8} , Matt Kirwan⁹ , Anya M. Hopple^{4,10}, and
J. Patrick Megonigal¹⁰ 

¹Marine and Coastal Research Laboratory, Pacific Northwest National Laboratory, Sequim, WA, USA, ²School of Oceanography, University of Washington, Seattle, WA, USA, ³Atmospheric Sciences and Global Change Division, Pacific Northwest National Laboratory, Richland, WA, USA, ⁴School of Biological Sciences, Washington State University, Pullman, WA, USA, ⁵Biological Sciences Division, Pacific Northwest National Laboratory, Richland, WA, USA, ⁶Joint Global Change Research Institute, Pacific Northwest National Laboratory, College Park, MD, USA, ⁷Now at School of Aquatic and Fishery Sciences, University of Washington, Seattle, WA, USA, ⁸Now at Institute of Mountain Hazards and Environment, Chengdu, China, ⁹Virginia Institute of Marine Science, Gloucester Point, VA, USA, ¹⁰Smithsonian Environmental Research Center, Edgewater, MD, USA

Abstract Methane (CH_4) exchange between trees and the atmosphere has recently emerged as an important, but poorly quantified process regulating global climate. The sources (soil and/or tree) and mechanisms driving the increase of CH_4 in trees and degassing to the atmosphere are inadequately understood, particularly for coastal forests facing increased exposure to seawater. We investigated the eco-physiological relationship between tree stem wood density, soil and stem oxygen saturation (an indicator of redox state), soil and stem CH_4 concentrations, soil and stem carbon dioxide (CO_2) concentrations, and soil salinity in five forests along the United States coastline. We aim to evaluate the mechanisms underlying greenhouse gas increase in trees and the influence of seawater exposure on stem CH_4 accumulation. Seawater exposure corresponded with decreased tree survival and increased tree stem methane. Tree stem wood density was significantly correlated with increased stem CH_4 in seawater exposed gymnosperms, indicating that dying gymnosperm trees may accumulate higher levels of CH_4 in association with seawater flooding. Further, we found that significant differences in seawater exposed and unexposed gymnosperm tree populations are associated with increased soil and stem CH_4 and CO_2 , indicating that seawater exposure significantly impacts soil and stem greenhouse gas abundance. Our results provide new insight into the potential mechanisms driving tree CH_4 accumulation within gymnosperm coastal forests.

Plain Language Summary Trees emit greenhouse gases such as methane and carbon dioxide to the atmosphere. The origin of these gases includes production in the tree or in the surrounding soils. Disturbances to these systems, such as seawater exposure that increases soil salinity, have an unknown impact on gas production and connectivity between soil and trees. We found that higher soil salinities corresponded to higher soil methane content and increased stem methane. The accumulation of soil and tree methane was lower in sites with no salinity exposure and higher in sites with high salinity. As coastal systems become more vulnerable to changes in seawater exposure, this may have consequences on methane emitted from trees to the atmosphere.

1. Introduction

Increasing atmospheric greenhouse gas (GHG) levels have resulted in polar warming that is projected to cause sea levels to rise substantially in the next century (de Coninck et al., 2018; Overpeck et al., 2006). The amount of methane (CH_4) in the atmosphere is increasing globally, representing an important positive feedback on climate warming that is regulated by numerous terrestrial and aquatic sources and sinks (Winterstein et al., 2019). Upland soils take up 30 Tg CH_4 yr^{-1} , freshwater wetlands emit \sim 150 Tg CH_4 yr^{-1} , and wetlands exposed to seawater (e.g., salt marshes) are thought to play a net neutral role in global CH_4 cycling (Poffenbarger et al., 2011; Saunois et al., 2016). Critical gaps in mechanistic understanding of how

Matt Kirwan, Anya M. Hopple, J.

Patrick Megonigal

Writing – review & editing: Matthew

J. Norwood, Nicholas D. Ward, Nate

G. McDowell, Allison N. Myers-Pigg,

Ben Bond-Lamberty, Julia Indivero,

Stephanie Pennington, Wenzhi Wang,

Matt Kirwan, Anya M. Hopple, J.

Patrick Megonigal

ecosystems exchange CH₄ to and from the atmosphere inhibit our ability to quantify present day cycling and future responses to ecosystem disturbances such as warming, sea level rise, and changes in precipitation (Bridgman et al., 2013). Considering CH₄ has a greenhouse gas warming potential 87–11 times greater than CO₂ over 20 to 500-year timescales (Neubauer & Megonigal, 2015), a mechanistic understanding of CH₄ cycling is necessary for a predictive outlook on ecosystem response to change.

Natural ecosystems are faced with a variety of anthropogenic disturbances that may dramatically shift their biogeochemical function (Fichtner et al., 2014) and coupling or decoupling of different ecosystem components (e.g., rhizosphere-tree stem) (Mark et al., 2005; Noe et al., 2011; Willig et al., 1996). Increased coastal forest inundation events such as due to rising sea level and increasing storm frequency (Fagherazzi et al., 2019; Lin et al., 2020; K. Williams et al., 2003; C. A. Williams et al., 2016), ultimately may turn forests that were net carbon sinks to net carbon sources (Hadden & Grelle, 2016). There have already been demonstrable changes in coastal ecosystems, with wetlands drowning and coastal forests dying (Kirwan & Gedan, 2019; W. Wang et al., 2019), and upland terrestrial ecosystems also feeling pressure from increasing drought/flood cycles and rising temperatures (McDowell et al., 2018).

Environmental disturbances such as freshwater flooding (Pangala et al., 2017; Pitz et al., 2018) and salt intrusion (Ward et al., 2019) are expected to increase either the production of GHGs within tree stems or the export of GHGs from soils to the atmosphere. Environmental changes and/or disturbances to forest soil CH₄ and CO₂ source or sink functions can be influenced by changes to soil temperature, soil moisture content, and soil biogeochemistry (Bowden et al., 1993; King, 1997; Ni & Groffman, 2018; Ojima et al., 1993; Raich & Schlesinger, 1992). Environmental changes and/or disturbances to these ecosystems can influence CH₄ and CO₂ net greenhouse gas budgets (Bousquet et al., 2006; Dlugokencky et al., 2011). However, these responses are neither understood from a mechanistic perspective nor easily measured across spatial scales broad enough to reveal continental-to global-scale patterns. Therefore, gaining a mechanistic understanding on the effects of coastal forest flooding on soil/tree GHG cycling is important in predicting climate-induced carbon feedbacks.

Global CH₄ budget estimates typically do not include an important pathway for gas exchange between soils and the atmosphere—CH₄ emissions from woody vegetation (Barba et al., 2019; Bousquet et al., 2006; Covey & Megonigal, 2019; Megonigal & Guenther, 2008). Nonwoody vegetation has long been recognized as playing an important role in wetland CH₄ exchange, yet little attention has been paid to the contributions of tree stems, despite the large surface area they represent in forested ecosystems (Crowther et al., 2015). The few examples in the literature have found that CH₄ emissions from tree stems are locally (Covey & Megonigal, 2019) and regionally relevant (Machacova et al., 2016; Pangala et al., 2017; Z. P. Wang et al., 2017), with the potential to offset the soil CH₄ sink by up to 63% (Covey & Megonigal, 2019). Furthermore, CH₄ emissions from trees represent a conduit for CH₄ to escape from deeper soil layers to the atmosphere in ecosystems that are often considered CH₄ sinks, such as upland forests (Carmichael et al., 2014; Covey et al., 2012; Le Mer & Roger, 2001) and coastal floodplain forests (Ward et al., 2019).

The magnitude of tree CH₄ exchange partially depends on the provenance of CH₄ (i.e., soil vs. tree sources), transport pathways and mechanisms (i.e., diffusion vs. mass flow), and drivers of gas diffusion rates (e.g., stem morphology and stem water content) (Barba et al., 2019; Megonigal et al., 2020). The extent to which CH₄ emissions from trees are coupled to soils will vary with each of these factors, which in turn are influenced by ecosystem disturbances. Flooding induced increases in soil saturation severely restricts exchange of oxygen (O₂) between the atmosphere, soil pore spaces, and tree pore spaces. Molecular O₂ is consumed rapidly by aerobic plant and microbial respiration in soil and tree stems and can only be replaced by atmospheric gas flux through soil and tree pore spaces. As these spaces fill with water, diffusion pathways are effectively blocked as O₂ diffusion rates decline 103-fold and O₂ concentrations subsequently decline (Boyer et al., 1997; Collin & Rasmussen, 1988). The development of hypoxic or anoxic conditions fundamentally alters the dominant pathways of microbial respiration, both in soils (Megonigal et al., 2003) and in tree stems (Covey & Megonigal, 2019), and negatively impacts the physiology of plants that are not flood tolerant.

Here we use a new approach to discern coupling and decoupling of soil and tree stem biogeochemistry in order to identify the mechanisms by which tree stems accumulate and emit CH₄ in response to seawater exposure. We measured tree stem wood density, concentrations of O₂, CO₂, and CH₄ internally in gymnosperm

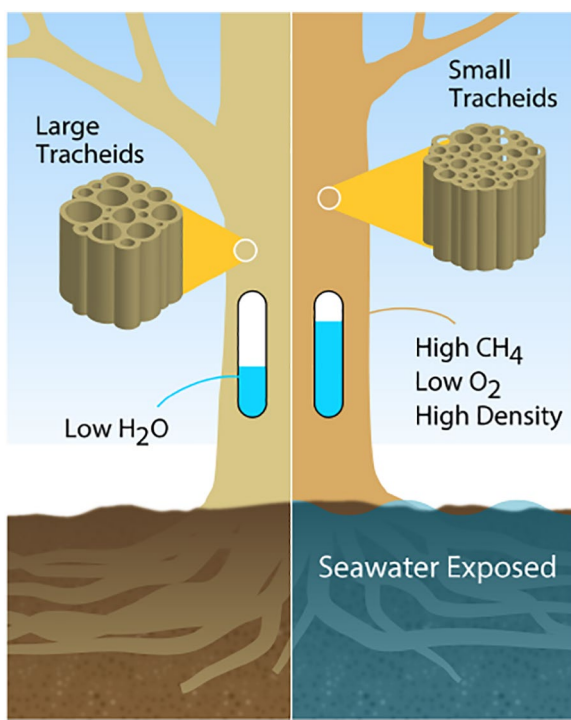


Figure 1. A conceptual diagram of the mechanisms driving soil-tree CH₄ exchange in seawater exposed coastal forests. Density can be affected by water content and/or tracheid size. Higher density results in higher internal stem CH₄ and limited O₂ diffusion.

Meinzer et al., 2008; Rinn et al., 1996). We sampled five gymnosperm coastal forests, with two randomized nominal plots at each site, containing living and dying trees for both seawater exposed and unexposed locations (Table 1; Figure 2). Three soil measurements were collected within each plot for soil salinity and soil gases.

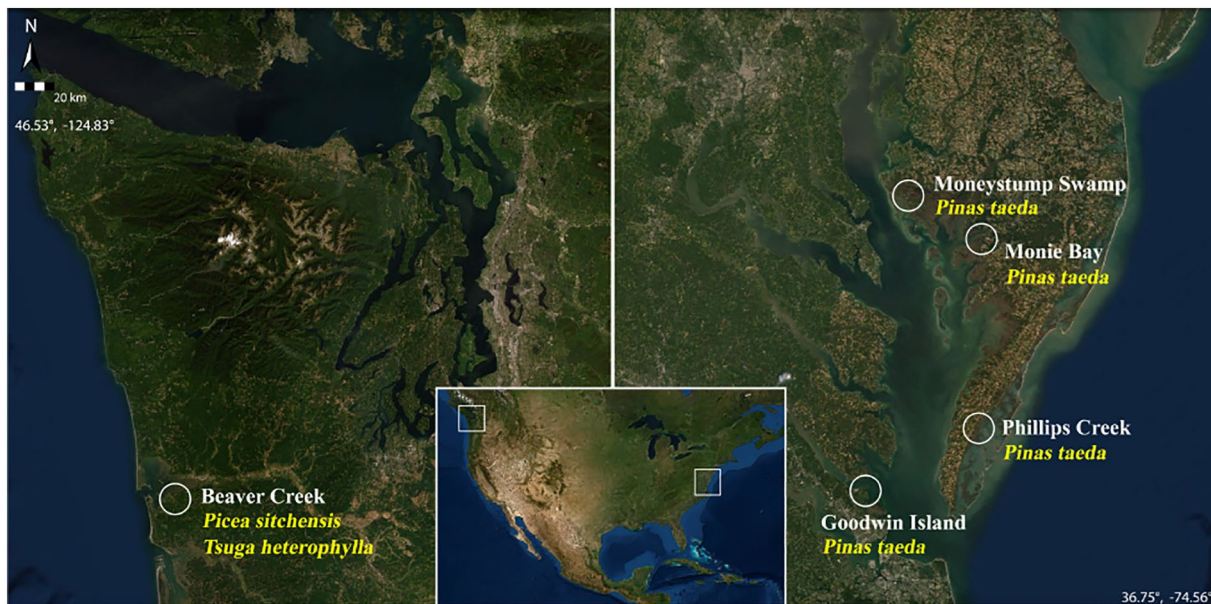


Figure 2. The five sites where trees and soils were sampled for percent O₂ and internal stem CO₂ & CH₄ concentrations. Sites are denoted with tree species. Map was created using ArcGIS 10.5 software (ESRI, 2017). Coordinate system: GCS WGS 1984.

tree stems (a method that has been previously used with CO₂ and O₂ to study tree respiration [Cerasoli et al., 2009; Teskey & McGuire, 2007; Teskey et al., 2008]) and in soil pore spaces (liquid or gaseous phase depending on soil saturation) and interpret these data in the context of seawater exposed trees and unexposed trees. First, we hypothesize that seawater exposure will increase internal gymnosperm-stem CH₄ and CO₂ concentrations, compared to unexposed trees (Figure 1). Second, we hypothesize that seawater exposure will significantly increase stem wood density, with increased stem wood density significantly correlated with increased stem CH₄ and CO₂. Finally, we hypothesize that seawater exposure will have a significant effect on stem and soil gases (CH₄, CO₂, and O₂), with the relationship between GHGs in seawater exposed trees and unexposed trees uniquely clustered in a multivariate space.

2. Materials and Methods

2.1. Study Sites

Measurements of soil and tree stem O₂, CO₂, and CH₄ concentrations were made at five sites representing two coastal eco-regions: the Mediterranean Pacific Northwest and the temperate Atlantic Eastern shore (Figure 2). In total, 107 trees were sampled, pairing stem and soil gas measurements for CO₂, CH₄, and O₂, and average stem wood density (Table 1 and Norwood, 2020). The number of trees by tree species, seawater exposure, and tree survival are represented in Table 1. All stem gas and bulk soil gas samples were collected during daylight hours during the 2019 growing season (late June—early September). All stem density measurements were made at breast height on the north-facing side of the stem to reduce variability between sun exposed wood versus shaded wood (Meinzer et al., 2008; Rinn et al., 1996).

We sampled five gymnosperm coastal forests, with two randomized nominal plots at each site, containing living and dying trees for both seawater exposed and unexposed locations (Table 1; Figure 2). Three soil measurements were collected within each plot for soil salinity and soil gases.

Table 1

Distribution of Tree Samples for each Location by Tree Species
(*n* = Total Number of Trees), Seawater Exposure (exp. = Exposed,
unx. = Unexposed), and Tree Survival (Living or Dying)

Location	Tree species	Exp.	Unx.	Living	Dying
Beaver Creek	<i>P. sitchensis</i> (<i>n</i> = 12)	12	0	6	6
	<i>T. heterophylla</i> (<i>n</i> = 6)	3	3	6	--
Goodwin Island	<i>P. taeda</i> (<i>n</i> = 35)	23	12	23	12
Phillips Creek	<i>P. taeda</i> (<i>n</i> = 18)	12	6	12	6
Monie Bay	<i>P. taeda</i> (<i>n</i> = 18)	12	6	12	6
Moneystump	<i>P. taeda</i> (<i>n</i> = 18)	12	6	13	5

Note. Tree survival was estimated by percent canopy greenness (Wang et al., 2019).

Each plot consisted of an area larger than 100 m², with soil measurements tied to each plot. Living and dying trees were randomly selected within each respective plot, with individual tree density and gas measurements recorded for each tree that was randomly selected within the plot.

Here we identify seawater exposure at each of the five sites (Figure 2). Beaver Creek, WA—a first order watershed with a previously freshwater swamp in its lowlands that became exposed to seawater inundation 5 years before sampling due to culvert removal and an undisturbed (non-flooded) upland forest (W. Wang et al., 2019). Beaver Creek is located in western Washington state (Pacific Northwest coast ecoregion). The climate in this region typically consists of dry summers and cool, wet winters, with a mean annual temperature of 10.4°C and an average annual precipitation of 1,640 mm from September to May (W. Wang et al., 2019; Ward et al., 2019). The Beaver Creek site includes two gymnosperm species, *Picea sitchensis* and *Tsuga heterophylla*, with 18 trees sampled total (12x *P. sitchensis* and 6x *T. heterophylla*).

Goodwin Island, Phillips Creek, Monie Bay, and Moneystump Swamp are coastal forest sites around Chesapeake Bay that are experiencing significant tree die off due to sea-level rise and nonflooded trees distal to shoreline (Kirwan & Gedan, 2019; Schieder & Kirwan, 2019; Schieder et al., 2018). Goodwin Island, Phillips Creek, Monie Bay, and Moneystump Swamp sites are located in a similar temperate climate, where naturally occurring stands of one gymnosperm species, *Pinus taeda*, are associated with coastal plain soils near tidal marshes (Brinson et al., 1995; Kirwan et al., 2007, 2016; Brush et al., 1980). Goodwin Island is located near Seaford, VA in the York River near the mouth of the Chesapeake Bay (Kirwan et al., 2016). Phillips Creek (Nassawadox, VA), Monie Bay (Venton, MD), and Moneystump Swamp (Golden Hill, MD) are located on the Delmarva Peninsula on the western shore of the Chesapeake Bay (Brinson et al., 1995; Kirwan et al., 2007). We sampled 89 *P. taeda* trees during early September 2019 (Table 1). Rhode River, Phillips Creek, Monie Bay, Goodwin Island, and Moneystump contain both nearshore forests that are flooded by seawater and higher elevation forests that are above the saline flood level. Within these sites, we sampled both the near shore seawater exposed forest and upland unexposed forests.

For this study, trees were sampled once during the growing season in late June 2019 at Beaver Creek and once in early September 2019 at Goodwin Island, Phillips Creek, Monie Bay, and Moneystump (Table 1). All the trees sampled in this study were estimated to be at mid-to late-growth stages, according to stem DBH threshold being greater than 13 cm (Blackwood et al., 2010; Shendryk et al., 2016).

2.2. Tree Density, Tree Gas and Soil Porewater Sampling Method

Average green-stem wood density measurements were recorded with an absolute density calibrated Rinn-tech Resistograph® R650-Sc (Rinn et al., 1996). Stem density was integrated across the stem at breast height. To measure stem concentrations of pCH₄ and pCO₂, we followed a similar protocol to that of Covey et al. (2012). Individual trees were cored with a 12-mm Haglof increment borer in which a stainless-steel pipe (0.493" [12.5 mm] inner diameter and 43/64" outer diameter [17.06 mm]) was inserted with a rubber septum seal (Suba Seal®) equipped for repeated gas sampling. Tree stem greenhouse gas samples were extracted at breast height via gas-tight syringe and needle (25 ml). Stem O₂ was measured with a Fire Sting O₂ Optimal Oxygen Meter (Pyroscience, Bremen, Germany). Stem O₂ saturation was normalized to atmospheric O₂ (20.95%).

We followed the methodology from Ward et al. (2019) to measure CH₄ and CO₂ concentrations in the soil porewater at each site, using a headspace extraction method with porewater from the soil. A 60-cm long, 3.175-mm-diameter stainless steel probe (M.H.E. Products Push Point Research Samplers) with small openings at the tip was inserted into three random locations within at each plot. A 60-mL syringe with a two-way Luer-lock valve was then used to draw out 20 mL of porewater from the soil probe. We used an additional syringe and a three-way Luer-lock valve to transfer 40 mL of pure N₂ gas to the sampling syringe. The syringe was shaken for approximately 2 min to equilibrate the gases in the water sample, allowed to settle, and then 40 mL of the headspace was removed in the second 60-mL syringe. Roughly 100 mL of porewater

was collected prior to GHG sampling to rinse the sampling probe and discard initial water with high turbidity. Samples were collected immediately after this rinse step. Rinse steps occurred over 3x the volume of the total porewater collection volume. Using the same sampling probe, we also measured porewater salinity, temperature, and dissolved oxygen using a YSI Pro Plus multiparameter sonde. In sites where porewaters were unable to be extracted, a 60-mL gas sample was taken through the soil probe and soil oxygen was measured with the Fire Sting GO₂ Optimal Oxygen Meter in the top 7 cm of soil.

Gas samples were collected into preevacuated glass vials and taken back to the lab for storage and analysis. Although gas samples were stored in gas tight vials, sample storage did not exceed 2-weeks from collection to analysis. Following the protocol described in Ward et al. (2019), gas samples were analyzed for the partial pressure of CO₂ and CH₄ (i.e., pGHG) by direct injection into a Picarro G2508 Cavity Ring-Down Spectrometer with a flow limiter installed on the inlet to reduce gas flow rates. Samples were diluted with N₂ when GHG levels were above the instrument's threshold. All concentration values are reported in μmol per liter of dry air ($\mu\text{mol L}^{-1}$). Porewater GHG values were corrected for dilution during headspace extraction and subsequent dilution prior to analysis based on the common gas law. Porewater gas concentrations were corrected for dissolution of gas in the water by converting to $\mu\text{mol L}^{-1}$ with Henry's law using temperature- and salinity-dependent coefficients (Wanninkhof, 2014):

$$\ln\beta = A_1 + A_2 * (100 / T) + A_3 * \ln(T / 100) + S * \left[B_1 + B_2 * (T / 100) + B_3 * (T / 100)^2 \right] \quad (1)$$

where β is the dimensionless Bunsen solubility coefficient, T is the temperature in °Kelvin, and S is the salinity in parts per thousand (or practical salinity units). A₁, A₂, A₃, B₁, B₂, and B₃ are gas-specific coefficients reported in Wanninkhof (2014).

2.3. Seawater Exposure Identification

Seawater exposure was assigned qualitatively in the field via visual identification of individual trees in the flooded zone, and quantitatively in the lab via measurements of the concentration of porewater salinity in porewater. We identified trees in higher elevations (distal to shoreline), as locations that do not experience frequent seawater inundation events. Soil salinity, soil O₂, soil CO₂, and soil CH₄ were measured at the plot level for each site. Trees located within a tidal flood zone plots, with saline porewaters higher than 0.10 (psu), were characterized as seawater exposed (n = 74). Trees classified as unexposed to seawater (n = 33), could however include disturbances outside of the scope of this study (e.g., pest infestation, nutrient enrichment, etc.) (Table 1).

2.4. Statistical Analysis

All significant thresholds were set to $p < 0.05$ and adjusted using Benjamini-Hochberg p-value correction, with a confidence interval of 95%. Wilcoxon signed-rank tests and Spearman linear relationships were tested between groups, where groups consisted of flooding type (seawater exposure) and tree survival (living or dying), defined by canopy cover (W. Wang et al., 2019). Factorial analysis of mixed data types (FAMD) was used to explore unique data clusters based upon input variables (including both numerical and categorical data). The numerical input variables (n = 6) include stem CO₂, stem CH₄, stem O₂, soil CH₄, soil CO₂, and soil O₂. The two categorical variables are seawater exposure and tree survival. Nonmetric multidimensional scaling with Euclidean distances was used to ordinate variables from the FAMD in 2-dimensional space ($k = 2$). Twenty random restarts were used to find a solution for the Euclidean distances along two axes. Bootstrapping with 999 permutations was used for group significance tests ($p < 0.01$). Homogeneity of the multivariate data was tested using analysis of variance for the output distances ($p = 0.60$). Both numerical and categorical data used for interpretation in this manuscript can be found in Norwood (2020).

The R packages used for data interpretation are freely available in R package version 0.8.3 and R 3.5.2 (RStudio Team, 2017). Original and adapted R codes used to run statistics and make figures are found in Table S1. All statistical tests were performed using R version 3.5.2 (RStudio Team, 2017); ggplot2 version 3.2.1 was used to make Figures 3–5 (Wickham et al.,). Factorial analysis of mixed data was performed with the factoextra R package version 1.0.5 (Kassambara & Mundt, 2017). Nonmetric multidimensional scaling was performed with the vegan package 2.5–6 (Oksanen et al., 2019).

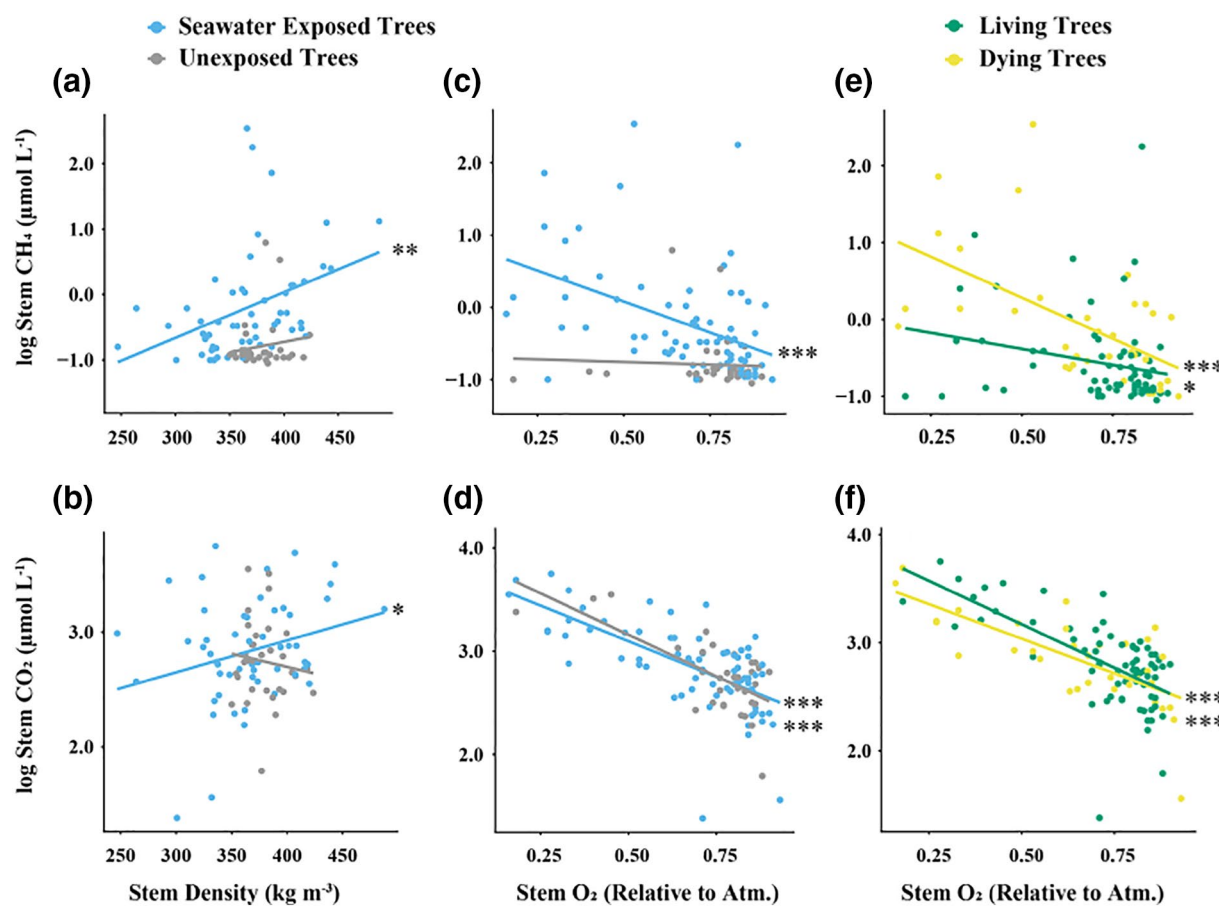


Figure 3. Scatterplots of tree stem $\log \text{CH}_4$ ($\mu\text{mol L}^{-1}$) and stem $\log \text{CO}_2$ ($\mu\text{mol L}^{-1}$) compared to average stem wood density (kg m^{-3}) (A & B, respectively) and stem O_2 (C-F, respectively). Stem O_2 is normalized to atmospheric O_2 (20.95%). Data is grouped by seawater exposure (a)–(d) and tree survival (e) & (f). Note Table 4 for significance statistics within the 95% confidence interval represented by *.

3. Results

3.1. Tree and Soil Mean Statistics

Mean stem wood density, stem CH_4 , stem CO_2 and stem O_2 was significantly different across the three different species (Table 2). *P. sitchensis* had significantly higher stem wood density, stem CH_4 , and significantly lower stem O_2 compared to the other two tree species (Table 2). Mean stem CH_4 was significantly higher for seawater exposed trees and dying trees (Table 2). Mean soil salinity, soil CH_4 , soil CO_2 and soil O_2 were significantly different for exposure type and tree survival; with seawater exposure and dying trees experiencing higher soil salinity, soil CH_4 , soil CO_2 and lower soil O_2 (Table 3).

3.2. Correlation Between Stem Wood Density, Stem GHGs, and Stem O_2

Seawater exposed trees had a significant positive linear relationship between stem CH_4 and stem wood density (Figure 3a & Table 3). Similarly, seawater exposed trees had a significant positive linear relationship between stem CO_2 and stem density (Figure 3b & Table 3). The linear relationship of both stem CH_4 and stem CO_2 has a significant negative linear relationship with stem O_2 for seawater exposed trees (Figures 3c and 3d & Table 3); with a significant negative linear relationship between stem CO_2 and O_2 (Figure 3d & Table 3).

Tree survival (living or dying) did not have a significant effect on the relationship between stem GHGs (CH_4 or CO_2) and stem wood density. Living and dying trees had a significant negative linear relationship between stem CH_4 and stem O_2 ; while only living trees had a significant negative linear relationship between stem CO_2 and stem O_2 (Figures 3e and 3f & Table 3).

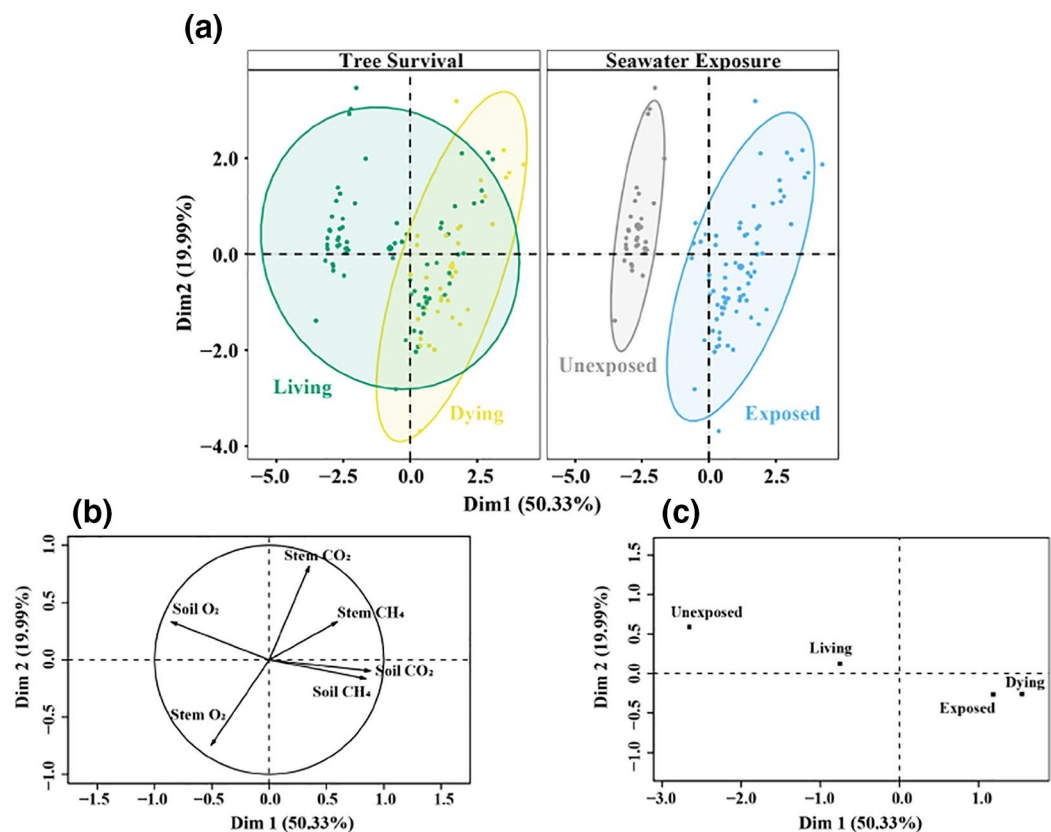


Figure 4. Factorial Analysis of Mixed Data Map (a) and distribution of quantitative variables (b). The quantitative variables include log stem CO₂ ($\mu\text{mol L}^{-1}$), log stem CH₄ ($\mu\text{mol L}^{-1}$), stem O₂, soil O₂, log soil CH₄ ($\mu\text{mol L}^{-1}$), and log soil CO₂ ($\mu\text{mol L}^{-1}$). The categorical variables (c) include tree survival (living or dying) and seawater exposure (exposed or unexposed).

3.3. Factorial Analysis of Mixed Data and Nonmetric Multidimensional Scaling

Factorial Analysis of Mixed Data (FAMD) was performed to evaluate how both qualitative information (i.e., tree survival [living or dying] and seawater exposure [exposed or unexposed]) and quantitative data (i.e., stem CO₂, stem CH₄, stem O₂, soil O₂, log soil CH₄ ($\mu\text{mol L}^{-1}$), and log soil CO₂ ($\mu\text{mol L}^{-1}$)). Dimensions one and two explained 70.32% of the variability in this data set (Figures 4a–4c). Dimension one explained 50.33% of the variation in our data, and was associated with soil O₂, soil CH₄, and soil CO₂; with soil O₂ having inverse relationship with soil GHGs along dimension one (Figure 4b). Dimension two explained 19.99% of the variation in our data, and was associated with stem O₂, stem CH₄, and stem CO₂; with stem O₂ having inverse relationship with stem GHGs along dimension two (Figure 4b). The categorical variables—tree survival and seawater exposure—were spread along dimensions one and two; with dying trees and seawater exposed trees clustering separately from unexposed-living trees (Figure 4c). Nonmetric multidimensional scaling (NMDS) was used to interpret multivariate data from the FAMD (i.e., seawater exposure, tree survival, stem CO₂, stem CH₄, stem O₂, soil CO₂, soil CH₄, and soil O₂). The NMDS model illustrates that there is a statistically significant difference between the seawater exposed gymnosperm trees and unexposed gymnosperm trees (Figure 5). The stress for the plot of variables in two-dimensions was 0.13 (Figure 5). Seawater exposure was a significant variable for stem and soil gases (CH₄, CO₂, and O₂ [$p < 0.01$]); while tree survival was not a significant variable ($p = 0.18$) (Figure 5).

Effects of Seawater Exposure on Tree & Soil GHG Accumulation

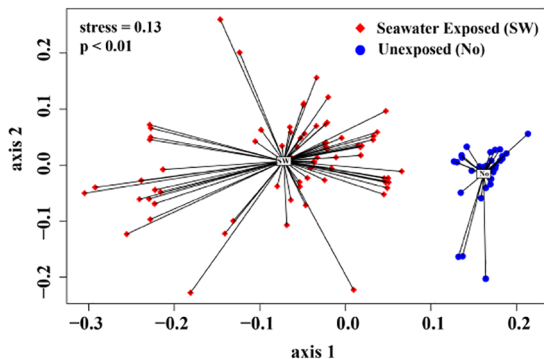


Figure 5. Nonmetric multidimensional scaling (NMDS) of quantitative variables and qualitative variables used in FAMD.

Table 2

Mean Comparison for Stem Wood Density (kg m^{-3}), Stem O_2 (Relative to Atmospheric [20.95]), Stem CH_4 ($\mu\text{mol L}^{-1}$), and Stem CO_2 ($\mu\text{mol L}^{-1}$) for Tree Species, Seawater Exposure (Exposed or Unexposed), and Tree Survival (Living or Dying) (Mean \pm Standard Error)

Type	Density (kg m^{-3})	Stem O_2 (Rel.)	Stem CH_4 ($\mu\text{mol L}^{-1}$)	Stem CO_2 ($\mu\text{mol L}^{-1}$)
<i>P. sitchensis</i> ($n_s = 12$)	413 ± 9.30	0.33 ± 0.03	9.69 ± 5.83	$2,214 \pm 372$
<i>T. heterophylla</i> ($n_s = 6$)	347 ± 14.8	0.43 ± 0.08	0.20 ± 0.05	$3,430 \pm 462$
<i>P. taeda</i>	366 ± 3.54	0.77 ± 0.01	7.01 ± 4.41	634 ± 42.7
Species	$H = 18.4, p < 0.001$	$H = 41.3, p < 0.001$	$H = 20.9, p < 0.001$	$H = 20.9, p < 0.001$
Exposed	366 ± 5.32	0.68 ± 0.02	9.83 ± 5.35	$1,049 \pm 123$
Unexposed	378 ± 3.20	0.76 ± 0.03	0.42 ± 0.21	786 ± 141
Exposure	$H = 0.37, p = 0.54$	$H = 1.33, p = 0.25$	$H = 29.2, p < 0.001$	$H = 0.29, p = 0.59$
Living	370 ± 3.68	0.73 ± 0.02	3.17 ± 2.50	956 ± 118
Dying	373 ± 8.42	0.66 ± 0.04	14.6 ± 3.58	991 ± 166
Survival	$H = 0.35, p = 0.56$	$H = 1.71, p = 0.19$	$H = 15.1, p < 0.001$	$H = 0.15, p = 0.70$

4. Discussion

Trees may play an important role in global climate regulation by transporting greenhouse gases such as methane (CH_4) and carbon dioxide (CO_2), into the atmosphere. As seawater exposure only began in the last few decades (or less) for trees located within the coastal forest sites sampled in this study, trees were likely not well adapted to seawater conditions. Increased stem CH_4 is significantly correlated to increased wood density in seawater exposed trees (i.e., positive linear relationship), which may be linked to increased stem water content and decreased tracheid size increasing the gas diffusion barrier between internal stem CH_4 and atmospheric CH_4 (Ståhl, 1988) (Figure 3). Furthermore, seawater exposure is linked to tree survival (W. Wang et al., 2019) and increased stem CH_4 concentration, with higher soil salinities associated with decreased tree survival and increased soil CH_4 (i.e., positive linear relationship, Figure 1). Dying trees were significantly linked to high salinity and low O_2 soils (Table 3), highlighting seawater flooding impacts on coastal forest soils, tree survival, and GHGs. The compounding effects of seawater exposure on coastal forests GHG exchange are likely linked to both soil and tree eco-physical mechanisms; such as soil-tree-stem gas diffusion barriers and soil redox environments (Covey & Megonigal, 2019; Megonigal, 2020; Warner et al., 2017).

A consistent pattern that emerged from this broad survey of stem gas concentrations was the negative relationship between stem O_2 and stem GHGs (CO_2 and CH_4). We interpret this pattern to be a consequence of physical limitations to gas diffusion rates arising from wood anatomical features that affect the volume and connectivity of intercellular spaces, and the fraction of intercellular spaces filled with either water or air. Although stem gas abundance has been studied in tree stems (Hietala et al., 2015; Teskey et al., 2008), to our knowledge, this is the first study to examine the relationship of internal stem CH_4 and O_2 abundance in seawater exposed gymnosperm trees. Factors that decrease the diffusion of gases sourced from inside the stem— CO_2 and CH_4 —will slow the efflux of these gases to the atmosphere and thereby increase their stem concentration. These same factors will slow the diffusion of gases sourced from the atmosphere— O_2 —and thereby lower their stem concentration. This is consistent with the observation that tree stem emissions of soil-sourced radon peaked during daylight, when stem water content was at its daily minimum (Megonigal et al., 2020). Because radon is neither produced or destroyed in soils or tree stems, we concluded that stem water content was regulating stem emissions of radon, CO_2 , and CH_4 , all of which were positively correlated in angiosperm trees (Megonigal et al., 2020). Our observations indicate that stem water content and/or wood structure/anatomy may also regulate O_2 diffusion into gymnosperm stems, with consequences for the potential of the stem to support conditions for methanogenesis and methanotrophy.

Stem O_2 concentrations varied widely from anoxic to hypoxic to fully oxic, a pattern that held across all categories of trees (Figure 3). While this is consistent with previous observations of low stem O_2 concentra-

Table 3

Mean Comparison for Soil O_2 (Relative to Atmospheric [20.95]), Soil CH_4 ($\mu mol\ L^{-1}$), Soil CO_2 ($\mu mol\ L^{-1}$), and Soil Salinity (psu) Seawater Exposure (Exposed or Unexposed) and Tree Survival (Living or Dying) (Mean \pm Standard Error)

Type	Soil O_2 (Rel.)	Soil CH_4 ($\mu mol\ L^{-1}$)	Soil CO_2 ($\mu mol\ L^{-1}$)	Soil salinity (psu)
Exposed	$0.31 \pm 0.04\ (n_s = 32)$	$58.1 \pm 17.6\ (n_s = 32)$	$722 \pm 65.6\ (n_s = 32)$	$11.3 \pm 0.83\ (n_s = 32)$
Unexposed	$0.95 \pm 0.01\ (n_s = 6)$	$0.14 \pm 0.03\ (n_s = 6)$	$109 \pm 25.5\ (n_s = 6)$	$0.00 \pm 0.00\ (n_s = 6)$
Exposure (df = 1)	$H = 49.6, p < 0.001$	$H = 50.3, p < 0.001$	$H = 56.2, p < 0.001$	$H = 69.6, p < 0.001$
Living	$0.60 \pm 0.08\ (n_s = 21)$	$32.1 \pm 17.2\ (n_s = 21)$	$441 \pm 90.1\ (n_s = 21)$	$6.00 \pm 1.42\ (n_s = 21)$
Dying	$0.32 \pm 0.06\ (n_s = 17)$	$56.9 \pm 24.7\ (n_s = 17)$	$722 \pm 91.2\ (n_s = 17)$	$11.6 \pm 1.15\ (n_s = 17)$
Survival (df = 1)	$H = 10.3, p < 0.01$	$H = 9.95, p < 0.01$	$H = 14.4, p < 0.001$	$H = 17.6, p < 0.001$

tions (Baxter et al.; Covey & Megonigal, 2019; Mugnai & Mancuso, 2010 and references therein), we show that trees subjected to seawater exposure also support a wide range of stem redox environments. Previous studies found that lowering stem O_2 from 10% to 5% (v/v) resulted in a 25% reduction in respiration (Spicer & Holbrook, 2007), indicating that stem redox environments may control stem physiological function. Although we did not directly measure soil redox in this study, it is likely that seawater exposed trees and unexposed trees are rooted in a range of redox environments that may influence stem and soil gas exchange. This suggests that one of the most robust predictors of methanogenesis— O_2 content—cannot be predicted from the categories of tree condition used here, although tree O_2 was a good predictor of stem CH_4 and CO_2 .

Seawater exposure has a significant effect on the amount of CH_4 accumulated within tree stems (Table 2). Small differences in linear relationships between stem CO_2 versus stem O_2 for seawater exposure (Figure 3d), suggests that stem CO_2 is tightly coupled to O_2 concentrations within the stem. Teskey and McGuire (2007) found that 34% of CO_2 released by respiring cells within the xylem remained within the tree stem, while a portion of efflux CO_2 from the stem to the atmosphere originated in the root system (Teskey & McGuire, 2007). This indicates that stem CO_2 increase is coupled to both soil and stem CO_2 pools and that stem CO_2 increase is likely governed by physiological tree mechanisms, such as internal stem respiration rates (Ryan et al., 1992).

Seawater exposure significantly increased stem CH_4 , soil CH_4 , soil CO_2 , and soil salinity. One explanation for this pattern is that high levels of soil water content lead to high levels of stem water content, which in turn cause low rates of gas diffusion out of both the soils and tree stems where they are produced. Furthermore, trees growing in wet soils could be venting soil produced CH_4 from deeper soil layers, thereby bypassing zones of CH_4 oxidation in shallower soil horizons (Gauci et al., 2019). Higher stem and soil CH_4 in seawater exposed environments compared to unexposed environments suggests that this can occur even in locations where soil CH_4 fluxes are expected to be low due to sulfate abundance (Poffenbarger et al., 2011; Seyfferth et al., 2020). Previous studies have shown that rotting wood has similar magnitudes of CH_4 emissions as local soils, suggesting that buried rotting wood could switch soil CH_4 oxidation to soil CH_4 efflux (Warner et al., 2017). This could be an alternative explanation to high stem and soil CH_4 in seawater exposed trees where trees are acting as a conduit for methylotrophic methanogenesis deeper in soils and transported to the tree stem via soil-root-stem pathway.

Stem variables show an orthogonal relation with soil variables, indicating that stem and soil variables are related to both seawater exposure and tree survival (Figure 4). Living and unexposed trees were strongly associated with soil and stem O_2 (Figure 4), while tree stem and soil GHGs had a strong orthogonal relationship with dying and seawater exposed trees (Figure 4). This is likely related to lower rates of soil methanogenesis in unexposed soils, but possibly also due to an increase in sulfate reduction within seawater exposed topsoil and sulfate uptake by tree roots located within soil rhizome layers (Ahmed et al., 2019; Rennenberg, 1999). Within anoxic environments, where SO_4^{2-} and nitrate (NO_3^-) are limited, the complete mineralization

Table 4

Mean Correlation Statistics for the Linear Relationship Between Average Stem Wood Density (kg m^{-3}), Stem O_2 (Relative to Atmospheric [20.95]), Log Stem CH_4 ($\mu\text{mol L}^{-1}$), Log Stem CO_2 ($\mu\text{mol L}^{-1}$) for Seawater Exposure (Exposed and Unexposed) and Tree Survival (Living or Dying). p -values are From Spearman Correlations

Treatment	Stem density: Stem CH_4	Stem density: Stem CO_2	Stem CH_4 : Stem O_2	Stem CO_2 : Stem O_2
Exposed (df = 72)	$R^2 = 0.16, p < 0.01$	$R^2 = 0.08, p < 0.05$	$R^2 = 0.20, p < 0.001$	$R^2 = 0.44, p < 0.001$
Unexposed (df = 31)	$R^2 = 0.02, p = 0.41$	$R^2 = 0.01, p = 0.51$	$R^2 = 0.01, p = 0.76$	$R^2 = 0.46, p < 0.001$
Living (df = 70)	$R^2 = 0.05, p = 0.09$	$R^2 = 0.02, p = 0.35$	$R^2 = 0.06, p = 0.05$	$R^2 = 0.44, p < 0.001$
Dying (df = 33)	$R^2 = 0.11, p = 0.10$	$R^2 = 0.08, p = 0.15$	$R^2 = 0.32, p < 0.001$	$R^2 = 0.51, p < 0.001$

of organic matter occurs via methanogenic fermentation (Le Mer & Roger, 2001; Megonigal et al., 2003). The link between soil CH_4 and soil O_2 is attributed to the soil redox environment, which reflects the favored substrates used for coupled reduction and oxidation processes in soil biogeochemical cycles. When soil CH_4 production is favored there is typically a depletion of other electron donors such as O_2 , Fe^{3+} , NO^{3-} , and SO_4^{2-} . In chronically seawater exposed environments (e.g., marshes), SO_4^{2-} is a more thermodynamically favorable electron donor, however this is not straight forward in terms of sporadic seawater exposed where flooding occurs in association to storm events and extreme high tides (Osman, 2013).

We found that seawater exposure significantly affects the abundance of both soil and stem GHGs, with distinct and significant differences in the effects of seawater exposure on soil and tree GHGs (Figure 5). Further, seawater exposure significantly decreases tree survival, with increased soil salinities significantly correlated to tree survival (Table 2). Disturbances that increase seawater or freshwater flooding have the potential to increase stem CH_4 emissions to the atmosphere through increased emissions from soil produced CH_4 , although major controls on stem gas emissions (i.e., gas diffusion barriers), may ultimately govern the magnitude of stem CH_4 emissions. Increased transport and emissions of soil gas through tree stems is caused by a steeper soil-atmosphere CH_4 concentration gradient and represents an increase in soil-tree-atmosphere coupling (Covey & Megonigal, 2019). Increased tree stem CH_4 concentrations in flooded environments may potentially increase the magnitude of stem CH_4 fluxes to the atmosphere from forest ecosystems (Pangala et al., 2013).

5. Conclusion

We found that seawater exposure is associated with increased soil and stem CH_4 and decreased tree survival. Increased stem CH_4 concentrations in response to coastal flooding suggests an increase in soil CH_4 flux through stems, which would short-circuit soil CH_4 oxidation and contribute to an overall increase in CH_4 emissions from the coastal forest ecosystems such as those impacted by sea level rise (Figure 1). Tree stem wood density may be a governing mechanism on the accumulation of greenhouse gases within tree stems, with seawater exposed trees containing significantly higher concentrations of stem CH_4 that is significantly correlated with increased wood density. Our results are based entirely on observational data, and thus these conclusions are tentative correlations only; confirmation and attribution of causation will require future testing in manipulative experiments. Future identification of at-risk coastal forests that will experience seawater exposure, and quantification of stem CH_4 emissions within coastal forests will aid in refinement of baseline coastal forest CH_4 fluxes to the atmosphere.

Data Availability Statement

All data supporting the analyses and conclusions of this study are presented in the figures, tables, and supporting information of this manuscript. The data used in this manuscript can be found in Norwood, M. (2020), Coastal Forest Seawater Exposure Increases Stem Methane Concentration Manuscript Data, HydroShare, <https://doi.org/10.4211/hs.17e9a223ffe64e768e6cb8b2a77c198d>.

Acknowledgments

The research described in this paper is part of the Open Call Initiative at the Pacific Northwest National Laboratory. It was conducted under the Laboratory Directed Research and Development Program at PNNL, a multiprogram national laboratory operated by Battelle for the U.S. Department of Energy. We thank the PNNL Marine Sciences Lab for access to the Sequim Bay field site. We thank Don Lentz, Hancock Timber Company, and WA Department of Fish & Wildlife for access to the Beaver Creek field site. We thank Tyler Messerschmidt, Alex Smith, and Krystal Krygowski for aid in field campaigns.

References

Ahmed, S., Kayes, I., Shahriar, S. A., Kabir, M. M., Salam, M. A., & Mukul, S. A. (2019). Global Journal of Environmental Science and Management Soil salinity and nutrients pattern along a distance gradient in coastal region. *Global Journal of Environmental Science and Management*, 6(1), 59–72. <https://doi.org/10.22034/gjesm.2020.01.05>

Barba, J., Bradford, M. A., Brewer, P. E., Bruhn, D., Covey, K., van Haren, J., et al. (2019). Methane emissions from tree stems: A new frontier in the global carbon cycle. *New Phytologist*, 222(1), 18–28. <https://doi.org/10.1111/nph.15582>

Blackwood, A., Kingsford, R., Nairn, L., & Rayner, T. (2010). *The effect of river red gum decline on woodland birds in the Macquarie Marshes*. Sydney, Australia: The Australian Rivers and Wetlands Centre.

Bousquet, P., Ciais, P., Miller, J. B., Dlugokencky, E. J., Hauglustaine, D. A., Prigent, C., et al. (2006). Contribution of anthropogenic and natural sources to atmospheric methane variability. *Nature*, 443(7110), 439–443. <https://doi.org/10.1038/nature05132>

Bowden, R. D., Castro, M. S., Melillo, J. M., Steudler, P. A., & Aber, J. D. (1993). Fluxes of greenhouse gases between soils and the atmosphere in a temperate forest following a simulated hurricane blowdown. *Biogeochemistry*, 21(2), 61–71.

Boyer, J. S., Wong, S. C., & Farquhar, G. D. (1997). CO₂ and water vapor exchange across leaf cuticle (epidermis) at various water potentials. *Plant Physiology*, 114(1), 185–191.

Bridgman, S. D., Cadillo-Quiroz, H., Keller, J. K., & Zhuang, Q. (2013). Methane emissions from wetlands: Biogeochemical, microbial, and modeling perspectives from local to global scales. *Global Change Biology*, 19(5), 1325–1346. <https://doi.org/10.1111/gcb.12131>

Brinson, M. M., Christian, R. R., & Blum, L. K. (1995). Multiple states in the sea-level induced transition from terrestrial forest to estuary. *Estuaries*, 18(4), 648–659. <https://doi.org/10.2307/1352388>

Brush, G. S., Lenk, C., & Smith, J. (1980). The Natural Forests of Maryland: An Explanation of the Vegetation Map of Maryland. *Ecological Monographs*, 50(1), 77–92. <http://dx.doi.org/10.2307/2937247>

Carmichael, M. J., Bernhardt, E. S., Bräuer, S. L., & Smith, W. K. (2014). The role of vegetation in methane flux to the atmosphere: Should vegetation be included as a distinct category in the global methane budget? *Biogeochemistry*, 119(1–3), 1–24. <https://doi.org/10.1007/s10533-014-9974-1>

Cerasoli, S., McGuire, M. A., Faria, J., Mourato, M., Schmidt, M., Pereira, J. S., et al. (2009). CO₂ efflux, CO₂ concentration and photosynthetic refixation in stems of Eucalyptus globulus (Labill.). *Journal of Experimental Botany*, 60(1), 99–105. <https://doi.org/10.1093/jxb/ern272>

Collin, M., & Rasmussen, A. (1988). A comparison of gas diffusivity models for unsaturated porous media. *Soil Science Society of America Journal*, 52(6), 1559–1565.

Covey, K. R., & Megonigal, J. P. (2019). Methane production and emissions in trees and forests. *New Phytologist*, 222(1), 35–51. <https://doi.org/10.1111/nph.15624>

Covey, K. R., Wood, S. A., Warren, R. J., Lee, X., & Bradford, M. A. (2012). Elevated methane concentrations in trees of an upland forest. *Geophysical Research Letters*, 39(15). <https://doi.org/10.1029/2012GL052361>

Crowther, T. W., Glick, H. B., Covey, K. R., Bettigole, C., Maynard, D. S., Thomas, S. M., et al. (2015). Mapping tree density at a global scale. *Nature*, 525(7568), 201–205. <https://doi.org/10.1038/nature14967>

de Coninck, H., Revi, A., Babiker, M., Bertoldi, P., Buckeridge, M., Cartwright, A., et al. (2018). *Chapter 4: Strengthening and implementing the global response. In: Global Warming of 1.5 °C an IPCC special report on the impacts of global warming of 1.5 °C above pre-industrial levels and related global greenhouse gas emission pathways, in the context of strengthening the global response to the threat of climate change*. Intergovernmental Panel on Climate Change.

Dlugokencky, E. J., Nisbet, E. G., Fisher, R., & Lowry, D. (2011). Global atmospheric methane: Budget, changes and dangers. *Philosophical Transactions of the Royal Society A: Mathematical, Physical and Engineering Sciences*, 369(1943), 2058–2072.

Fagherazzi, S., Anisfeld, S. C., Blum, L. K., Long, E. V., Feagin, R. A., Fernandes, A., et al. (2019). Sea level rise and the dynamics of the marsh-upland boundary. *Frontiers in Environmental Science*, 7, 25.

Fichtner, A., Von Oheimb, G., Härdtle, W., Wilken, C., & Gutzknecht, J. L. M. (2014). Effects of anthropogenic disturbances on soil microbial communities in oak forests persist for more than 100 years. *Soil Biology and Biochemistry*, 70, 79–87.

Gauci, V., Pangala, S. R., Enrich-Prast, A., Gedney, N., Stauffer, T., Figueiredo, V., & Bastviken, D. (2019). Seasonal variability of tree methane emissions in the Central Amazon floodplain. *AGUFM*, 2019, B24B02.

Hadden, D., & Grelle, A. (2016). Changing temperature response of respiration turns boreal forest from carbon sink into carbon source. *Agricultural and Forest Meteorology*, 223, 30–38.

Hietala, A. M., Dörsch, P., Kvaalen, H., & Solheim, H. (2015). Carbon dioxide and methane formation in Norway spruce stems infected by white-rot fungi. *Forests*, 6(9), 3304–3325. <https://doi.org/10.3390/f6093304>

Kassambara, A., & Mundt, F. (2017). Package ‘factoextra’. In A. Kassambara (Ed.), *Extract and visualize the results of multivariate data analyses* (Vol. 76).

King, G. (1997). Responses of atmospheric methane consumption by soils to global climate change. *Global Change Biology*, 3(4), 351–362.

Kirwan, M. L., & Gedan, K. B. (2019). Sea-level driven land conversion and the formation of ghost forests. *Nature Climate Change*, 9(6), 450–457. <https://doi.org/10.1038/s41558-019-0488-7>

Kirwan, M. L., Kirwan, J. L., & Copenheaver, C. A. (2007). Dynamics of an estuarine forest and its response to rising sea level. *Journal of Coastal Research*, 232, 457–463. <https://doi.org/10.2112/04-0211.1>

Kirwan, M. L., Walters, D. C., Reay, W. G., & Carr, J. A. (2016). Sea level driven marsh expansion in a coupled model of marsh erosion and migration. *Geophysical Research Letters*, 43(9), 4366–4373. <https://doi.org/10.1002/2016GL068507>

Le Mer, J., & Roger, P. (2001). Production, oxidation, emission and consumption of methane by soils: A review. *European Journal of Soil Biology*, 37(1), 25–50. [https://doi.org/10.1016/S1164-5563\(01\)01067-6](https://doi.org/10.1016/S1164-5563(01)01067-6)

Lin, T.-C., Hogan, J. A., & Chang, C.-T. (2020). Tropical cyclone ecology: A scale-link perspective. *Trends in Ecology & Evolution*, 35(7), 594–604. <https://doi.org/10.1016/j.tree.2020.02.012>

Machacova, K., Bäck, J., Vanhatalo, A., Halmeenmäki, E., Kolari, P., Mammarella, I., et al. (2016). Pinus sylvestris as a missing source of nitrous oxide and methane in boreal forest. *Scientific Reports*, 6(1). <http://dx.doi.org/10.1038/srep23410>

Mark, G. L., Dow, J. M., Kiely, P. D., Higgins, H., Haynes, J., Baysse, C., et al. (2005). Transcriptome profiling of bacterial responses to root exudates identifies genes involved in microbe-plant interactions. *Proceedings of the National Academy of Sciences*, 102(48), 17454–17459.

McDowell, N. G., Michaletz, S. T., Bennett, K. E., Solander, K. C., Xu, C., Maxwell, R. M., & Middleton, R. S. (2018). Predicting chronic climate-driven disturbances and their mitigation. *Trends in Ecology and Evolution*, 33(1), 15–27. <https://doi.org/10.1016/j.tree.2017.10.002>

Megonigal, J. P., Brewer, P. E., & Knee, K. L. (2020). Radon as a natural tracer of gas transport through trees. *New Phytologist*, 225(4), 1470–1475. <https://doi.org/10.1111/nph.16292>

Megonigal, J. P., & Guenther, A. B. (2008). Methane emissions from upland forest soils and vegetation. *Tree Physiology*, 28(4), 491–498. <https://doi.org/10.1093/treephys/28.4.491>

Megonigal, J. P., Hines, M. E., & Visscher, P. T. (2003). *Anaerobic metabolism: Linkages to trace gases and aerobic processes*. In H. D. Holland, & G. Turekian (Eds.), *Treatise on geochemistry* (8–9, pp. 317–424). Oxford, UK: Pergamon. <https://doi.org/10.1016/B0-08-043751-6/08132-9>

Meinzer, F. C., Campanello, P. I., Domec, J. C., Gatti, M. G., Goldstein, G., Villalobos-Vega, R., & Woodruff, D. R. (2008). Constraints on physiological function associated with branch architecture and wood density in tropical forest trees. *Tree Physiology*, 28(11), 1609–1617.

Mugnai, S., & Mancuso, S. (2010). Oxygen transport in the sapwood of trees. In S. Mancuso & S. Shabala (Eds.), *Waterlogging signalling and tolerance in plants*. (pp. 61–75). Berlin, Heidelberg: Springer Berlin Heidelberg. https://doi.org/10.1007/978-3-642-10305-6_4

Neubauer, S. C., & Megonigal, J. P. (2015). Moving beyond global warming potentials to quantify the climatic role of ecosystems. *Ecosystems*, 18(6), 1000–1013. <https://doi.org/10.1007/s10021-015-9879-4>

Ni, X., & Groggman, P. M. (2018). Declines in methane uptake in forest soils. *Proceedings of the National Academy of Sciences*, 115(34), 8587–8590.

Noe, S. M., Kimmel, V., Hüve, K., Copolovici, L., Portillo-Estrada, M., Püttsepp, Ü., et al. (2011). Ecosystem-scale biosphere–atmosphere interactions of a hemiboreal mixed forest stand at Järvselja, Estonia. *Forest Ecology and Management*, 262(2), 71–81.

Norwood, M. (2020). *Coastal forest seawater exposure increases stem methane concentration manuscript data, HydroShare*. Retrieved from <https://doi.org/10.4211/hs.17e9a223ff64e768e6cb8b2a77c198d>

Ojima, D. S., Valentine, D. W., Mosier, A. R., Parton, W. J., & Schimel, D. S. (1993). Effect of land use change on methane oxidation in temperate forest and grassland soils. *Chemosphere*, 26(1–4), 675–685.

Oksanen, J., Guillaume, F., Blanchet, F. M., Kindt, R., Legendre, P., McGlinn, D., et al. (2019). *Vegan: Community ecology package*. R package version 2.5–6

Osman, K. T. (2013). Wetland soils. In K. T. Osman (Ed.), *Soils* (pp. 215–227). New York, NY; London, UK: Springer, Dordrecht.

Overpeck, J. T., Otto-Bliesner, B. L., Miller, G. H., Muhs, D. R., Alley, R. B., & Kiehl, J. T. (2006). Paleoclimatic evidence for future ice-sheet instability and rapid sea-level rise. *Science*, 311(5768), 1747–1750. <https://doi.org/10.1126/science.1115159>

Pangala, S. R., Enrich-Prast, A., Basso, L. S., Peixoto, R. B., Bastviken, D., Hornbrook, E. R. C., et al. (2017). Large emissions from floodplain trees close the Amazon methane budget. *Nature*, 552(7684), 230–234. <https://doi.org/10.1038/nature24639>

Pangala, S. R., Moore, S., Hornbrook, E. R. C., & Gauci, V. (2013). Trees are major conduits for methane egress from tropical forested wetlands. *New Phytologist*, 197(2), 524–531. <https://doi.org/10.1111/nph.12031>

Pitz, S. L., Megonigal, J. P., Chang, C.-H., & Szlavecz, K. (2018). Methane fluxes from tree stems and soils along a habitat gradient. *Biogeochemistry*, 137(3), 307–320. <http://dx.doi.org/10.1007/s10533-017-0400-3>

Poffenbarger, H. J., Needelman, B. A., & Megonigal, J. P. (2011). Salinity influence on methane emissions from tidal marshes. *Wetlands*, 31(5), 831–842. <https://doi.org/10.1007/s13157-011-0197-0>

Raich, J. W., & Schlesinger, W. H. (1992). The global carbon dioxide flux in soil respiration and its relationship to vegetation and climate. *Tellus B: Chemical and Physical Meteorology*, 44(2), 81–99.

Rennenberg, H. (1999). The significance of ectomycorrhizal fungi for sulfur nutrition of trees. *Plant and Soil*, 215(2), 115–122. <https://doi.org/10.1023/A:1004459523021>

Rinn, F., Schweingruber, F. H., & Schär, E. (1996). Resistograph and x-ray density charts of wood. Comparative evaluation of drill-resistance profiles and x-ray density charts of different wood species. *Holzforschung*, 50(4), 303–311.

RStudio Team. (2017). *RStudio: Integrated development environment for R*. Boston, MA: RStudio, Inc. Retrieved from <http://www.rstudio.com/>

Ryan, M. G., & Waring, R. H. (1992). Maintenance respiration and stand development in a subalpine lodgepole pine forest. *Ecology*, 73(6), 2100–2108.

Saunois, M., Bousquet, P., Poulter, B., Peregon, A., Ciais, P., Canadell, J. G., et al. (2016). The global methane budget 2000–2012. *Earth System Science Data*, 8(2), 697–751. <https://doi.org/10.5194/essd-8-697-2016>

Schieder, N. W., & Kirwan, M. L. (2019). Sea-level driven acceleration in coastal forest retreat. *Geology*, 47(12), 1151–1155. <https://doi.org/10.1130/G46607.1>

Schieder, N. W., Walters, D. C., & Kirwan, M. L. (2018). Massive upland to wetland conversion compensated for historical marsh loss in Chesapeake Bay, USA. *Estuaries and Coasts*, 41(4), 940–951. <https://doi.org/10.1007/s12237-017-0336-9>

Seyfferth, A. L., Bothfeld, F., Vargas, R., Stuckey, J. W., Wang, J., Kearns, K., et al. (2020). Spatial and temporal heterogeneity of geochemical controls on carbon cycling in tidal salt marsh. *Geochimica et Cosmochimica Acta*, 282, 1–18.

Shendryk, I., Broich, M., Tulbure, M. G., & Alexandrov, S. V. (2016). Bottom-up delineation of individual trees from full-waveform airborne laser scans in a structurally complex eucalypt forest. *Remote Sensing of Environment*, 173, 69–83.

Spicer, R., & Holbrook, N. M. (2007). Effects of carbon dioxide and oxygen on sapwood respiration in five temperate tree species. *Journal of Experimental Botany*, 58(6), 1313–1320.

Ståhl, E. G. (1988). *Transfer effects and variations in basic density and tracheid length of Pinus sylvestris L. populations (No 180)*. Faculty of Forestry, Swedish University of Agricultural Sciences. Retrieved from <http://urn.kb.se/resolve?urn=urn:nbn:se:slu:epsilon-9-16>

Teskey, R. O., & McGuire, M. A. (2007). Measurement of stem respiration of sycamore (*Platanus occidentalis* L.) trees involves internal and external fluxes of CO₂ and possible transport of CO₂ from roots. *Plant, Cell and Environment*, 30(5), 570–579. <https://doi.org/10.1111/j.1365-3040.2007.01649.x>

Teskey, R. O., Saveyn, A., Steppé, K., & McGuire, M. A. (2008). Origin, fate and significance of CO₂ in tree stems. *New Phytologist*, 177(1), 17–32. <https://doi.org/10.1111/j.1469-8137.2007.02286.x>

Wang, Z. P., Han, S. J., Li, H. L., Deng, F. D., Zheng, Y. H., Liu, H. F., & Han, X. G. (2017). Methane production explained largely by water content in the heartwood of living trees in upland forests. *Journal of Geophysical Research: Biogeosciences*, 122(10), 2479–2489. <https://doi.org/10.1002/2017JG003991>

Wang, W., McDowell, N. G., Ward, N. D., Indivero, J., Gunn, C., & Bailey, V. L. (2019). Constrained tree growth and gas exchange of sea-water-exposed forests in the Pacific Northwest, USA. *Journal of Ecology*, 107(6), 2541–2552. <https://doi.org/10.1111/1365-2745.13225>

Wanninkhof, R. (2014). Relationship between wind speed and gas exchange over the ocean revisited. *Limnology and Oceanography: Methods*, 12, 351–362. <https://doi.org/10.4319/lom.2014.12.351>

Ward, N. D., Indivero, J., Gunn, C., Wang, W., Bailey, V., & McDowell, N. G. (2019). Longitudinal gradients in tree stem greenhouse gas concentrations across six Pacific Northwest coastal forests. *Journal of Geophysical Research: Biogeosciences*, 124(6), 1401–1412. <https://doi.org/10.1029/2019JG005064>

Warner, D. L., Villarreal, S., McWilliams, K., Inamdar, S., & Vargas, R. (2017). Carbon dioxide and methane fluxes from tree stems, coarse woody debris, and soils in an upland temperate forest. *Ecosystems*, 20(6), 1205–1216.

Wickham, H., Averick, M., Bryan, J., Chang, W., McGowan, L., François, R., et al. (2019). Welcome to the tidyverse. *Journal of Open Source Software*, 4(43), 1686.

Williams, C. A., Gu, H., MacLean, R., Masek, J. G., & Collatz, G. J. (2016). Disturbance and the carbon balance of US forests: A quantitative review of impacts from harvests, fires, insects, and droughts. *Global and Planetary Change*, 143, 66–80.

Williams, K., MacDonald, M., & Sternberg, L. S. L. (2003). Interactions of storm, drought, and sea-level rise on coastal forest: A case study. *Journal of Coastal Research*, 19(4), 1116–1121.

Willig, M. R., Moorhead, D. L., Cox, S. B., & Zak, J. C. (1996). Functional diversity of soil bacterial communities in the tabonuco forest: Interaction of anthropogenic and natural disturbance. *Biotropica*, 28(4), 471–483.

Winterstein, F., Tanalski, F., Jöckel, P., Dameris, M., & Ponater, M. (2019). Implication of strongly increased atmospheric methane concentrations for chemistry-climate connections. *Atmospheric Chemistry and Physics*, 19(10), 7151–7163. <https://doi.org/10.5194/acp-19-7151-2019>